

Functorial invariants for chaos topology from data

Denisse Sciamarella*

*Institut Franco-Argentin d'Études sur le Climat et ses Impacts (CNRS – IRD – CONICET – UBA)
(IRL 3351 IFAECI), C1428EGA Ciudad Autónoma de Buenos Aires, Argentina and
CNRS – Centre National de la Recherche Scientifique, 75016 Paris, France*

(Dated: February 24, 2026)

The *templex* is a recently introduced topological object bridging homologies and templates for chaotic attractors: its cell complex encodes the directionless properties of the attractor's branched manifold in phase space, and its directed graph captures the flow-compatible paths starting and ending in joining loci. Algebraic topology is deeply connected to category theory because it studies spaces by translating them into algebraic objects through structure-preserving mappings. The homology functor translates structural properties into a set of layered invariants called homology groups. The *templex* is shown here to play the same role for directed spaces that cell complexes play for spaces. The directed properties of a *templex* are found therewith to admit a functorial formulation. This formulation provides a rigorous foundation for a theory of chaos topology developed so far algorithmically, and establishes operationally a topological criterion for finite-time chaos. A climatic simulation and an experimental speech signal are analyzed as illustrative applications.

I. INTRODUCTION

Understanding chaotic dynamics from trajectory data has traditionally required two steps: reconstructing orbits in phase space, and then describing how they wind around one another using braids, knots, or linking numbers [1, 2]. This approach is effective in three dimensions for low-noise datasets, but becomes impractical as soon as orbits cannot be reliably recovered from point clouds, as well as in higher-dimensional dynamics, where knots generically unknot. Several attempts have explored how to extend knot-holders, also called templates, beyond three dimensions, and move away from knot-based descriptions [3, 4].

A different approach bypasses orbit reconstruction altogether by working directly with the structure that supports a point cloud in phase space. This approach led to the construction of a cell complex designed to cling to attractors [5, 6], later dubbed Branched Manifold Analysis through Homologies (BraMAH) [7]. This type of cell complex allows one to compute homology groups of the supporting manifold with integer coefficients, retaining generators, orientability chains, and branching loci.

Classical algebraic topology, however, describes only the *structure* of a space, without accounting for how that structure is actually visited by a flow. Causality is ignored, and the mere existence of a hole does not imply that the flow circulates around it, nor that a folding without tearing — as in the spiral Rössler attractor — can be detected through homology alone. To incorporate the causal organization of a flow one must move from topology to *directed topology* [8–11], and from cell complexes to *templexes* [12–14].

A *templex* combines a BraMAH complex with a directed graph defined on its top-dimensional cells, encoding the flow-compatible transitions over the manifold and

how these paths organize themselves around *joining loci*. These elements allow us to introduce an (i) algebra of directed paths, (ii) a boundary-like operator acting on the set of all finite formal concatenations of directed edges, and (iii) a quotient of directed cycles modulo the image of this operator. The *templex* properties, which were previously defined and extracted algorithmically, can thus be endowed with the structure of directed spaces.

This structure opens the possibility of inscribing the *templex* within the framework of category theory [15, 16], and providing a functorial formulation for its directed invariants. Category theory describes mathematical structures in terms of objects and the arrows that represent morphisms between them; for instance, the category **Top** consists of topological spaces and continuous maps, while **Ab** consists of abelian groups and group homomorphisms. In chaos topology, homology groups are complemented by what we will call *generatex semigroups*. These concepts are illustrated through an experimental and a numerical example from speech [5] and the climate sciences [17], respectively.

II. THE TEMPLEX: DEFINITIONS

This section introduces mathematical definitions of the *templex* that generalize earlier constructions and place previously algorithmic procedures within a rigorous framework.

We first recall standard notions from homology theory. Next, we provide an intrinsic definition of a BraMAH complex. Finally, we describe how we incorporate causality.

A. Homologies

A *cell complex* is a topological space built by gluing cells of increasing dimension (points, segments, disks, and

* denisse.sciamarella@cnrs.fr

higher-dimensional analogues) along their boundaries. It provides a discrete, combinatorial representation of an underlying geometric object, and can be regarded as a topological *scaffold*: while the complex itself is not the object of interest, it supports algebraic constructions that reveal intrinsic properties of the space it represents. The *dimension* of a cell complex is defined as the highest dimension of its cells.

Given a finite cell complex K , the group of k -chains $C_k(K)$ is defined as the free abelian group generated by the k -cells of K ,

$$C_k(K) = \left\{ \sum_i n_i \sigma_i^k \mid n_i \in \mathbb{Z}, \sigma_i^k \text{ a } k\text{-cell of } K \right\},$$

together with a boundary operator

$$\partial_k : C_k(K) \longrightarrow C_{k-1}(K),$$

defined by assigning to each k -cell the formal sum of its $(k-1)$ -dimensional faces, with integer coefficients determined by their relative orientations.

The graded family of chain groups together with the boundary operators $\partial_k : C_k(K) \rightarrow C_{k-1}(K)$ that satisfy $\partial_{k-1} \circ \partial_k = 0$ is denoted by $C_\bullet(K) = \{C_k(K)\}_{k \geq 0}$. The group of k -cycles is the subgroup

$$Z_k(K) = \ker \partial_k \subset C_k(K),$$

while the group of k -boundaries is the subgroup

$$B_k(K) = \text{im } \partial_{k+1} \subset Z_k(K).$$

The k -th homology group is then defined as the quotient

$$H_k(K) = Z_k(K) / B_k(K).$$

Intuitively, forming a quotient amounts to identifying objects that play the same structural role across different representations. A useful metaphor is that of musical notes: D3 and D4 are distinct pitches, separated by an octave, yet both belong to the same note class ‘‘D’’, which might be known to some readers as ‘‘Re.’’ In homology, cycles that differ only by the attached higher-dimensional cells are identified in an analogous way, as they represent the same topological feature.

The generators of $H_k(K)$ correspond to intrinsic k -dimensional holes of the underlying space: they represent closed k -cycles that cannot be expressed as the boundary of any $(k+1)$ -dimensional chain. In this sense, homology detects topological features that are invariant under changes of the cell decomposition, capturing global properties such as connected components (0-holes), tunnels (1-holes), and higher-dimensional cavities ($k \geq 2$). A generator of $H_k(K)$ can be represented by any closed k -cycle within its equivalence class.

B. BraMAH complex

Cell complexes can be of different types depending on the construction rules used to build them from a point

cloud. A BraMAH complex is designed so that the topology of a (branched) manifold underlying a point cloud in phase space can be faithfully described by a single cell complex whose dimension coincides with that of the underlying manifold [5–7]. Here, a branched manifold is understood as a space that is locally a manifold almost everywhere [2].

In Ref. [13], a BraMAH complex of dimension h is defined as a cell complex constructed from a point cloud embedded in an n -dimensional phase space, with cells of dimension $k \leq h$, such that: (i) the 0-cells are a sparse subset of the original cloud of points in phase space; (ii) $h = d$, where $d \leq n$ is the intrinsic dimension of the underlying branched manifold being sampled; and (iii) each h -cell is such that h of the singular values that describe the distribution of the points around the barycenter of the cell scale linearly with the number of points in the cell [5, 6].

A BraMAH complex can be defined independently of algorithmic implementations as a finite cell complex \mathcal{B} whose geometric realization $|\mathcal{B}|$ is a manifold or a branched manifold, such that for each point $x \in |\mathcal{B}|$ there exists an integer $\kappa(x)$ —the local topological dimension—for which a neighborhood of x is homeomorphic to an open subset of $\mathbb{R}^{\kappa(x)}$. A cell is said to be top-dimensional if it is not a face of any cell of strictly higher dimension in the complex, even if its dimension is not maximal globally. A *junction locus* is a subcomplex where three or more top-dimensional cells meet along cells of lower dimension, assuming a minimal local cell structure; see Ref. [12] for details. These are the loci where a branched manifold fails to be a manifold.

Computing homology groups for a BraMAH complex provides an algebraic translation of the topological properties of the *structure* of a possibly branched manifold sampled by a point cloud in phase space. The zeroth homology group H_0 detects the number of connected components of the sampled support, indicating whether the system explores a single connected region of phase space or several disconnected ones. Homology groups of degree $k \geq 1$ capture higher-dimensional features, corresponding to regions of phase space avoided by the data and translating into voids of the support [5–7, 18].

Unlike constructions commonly used in persistent homology [19], the structure of a BraMAH complex does not depend on any filtration parameter. Top-cells can gather large subsets of points sampling the local topological structure of the manifold. This yields a topologically faithful cell complex, in which all topological information is preserved within a single unified structure, thus facilitating the computation of homology groups with integer coefficients, as well as extra information such as junction loci or orientability chains.

C. Templex

While homology captures the global structure of the set sampled in phase space, it is insensitive to temporal ordering. Let \mathcal{B} be a BraMAH complex, and let

$$\mathcal{G} = (V, E)$$

be a directed graph, or *digraph*, whose nodes V correspond one-to-one with the top-cells of \mathcal{B} , encoding the flow-compatible connections between them. The pair

$$\mathcal{T} = (\mathcal{B}, \mathcal{G})$$

defines a *templex*.

Once the digraph \mathcal{G} is taken into account, the junction locus, previously defined as a subcomplex of \mathcal{B} , naturally induces a subtemplex of \mathcal{T} whose top-cells can be identified as *ingoing* or *outgoing* according to the direction of the semi-flow across the lower-dimensional cell forming the junction. An *ingoing cell* (resp. *outgoing cell*) may therefore be referred to equivalently as an *ingoing node* (resp. *outgoing node*). Following the terminology introduced in template theory and used throughout previous works [12, 17], junction loci with a single ingoing node are called *splitting loci*, while those with a single outgoing node are called *joining loci*.

A *generatex* is a subtemplex whose subgraph is a directed cycle of \mathcal{G} . It is said to be of order p with $p \in \mathbb{N}$, $p \geq 1$, if the cycle has p distinct ingoing nodes. A generatex of order 1 is a stripex and a generatex of order $p > 1$ can be decomposed into p stripexes. Stripexes provide the direct bridge back to strips in the template tradition.

By construction, a templex necessarily contains intersections between generatexes. We define a *bond* as a connected subtemplex of \mathcal{T} on which the set of intersecting generatexes is fixed. For indices i_1, \dots, i_m with $m \geq 2$, such a bond is denoted by

$$B_{i_1 \dots i_m} = G_{i_1} \cap \dots \cap G_{i_m}.$$

Notice that the templex deliberately avoids resolving stratification within the top-cells. Its aim is to characterize the organization of the support, independently of metric features, which are captured by other types of invariants (e.g. fractal dimension). It is worth recalling that fractal dimension may take very similar values for attractors whose templex properties are fundamentally different.

III. ALGEBRA OF DIRECTED PATHS

Following classical homology, this section develops an algebra of directed paths for a templex, conceived as the analogue of the algebra of chains for a cell complex.

A. Concatenation

Let $\mathcal{T} = (\mathcal{B}, \mathcal{G})$ be a templex and let $C_{\mathcal{G}}(\mathcal{T})$ denote the set of all finite formal concatenations of directed edges of \mathcal{G} . Concatenation defines an associative product, so that for any three paths p, q, r ,

$$(pq)r = p(qr).$$

As direction matters in a templex, $C_{\mathcal{G}}(\mathcal{T})$ has the structure of a semigroup.

B. Poincaré edges

Among the directed edges of a templex there are special ones: those connecting several ingoing nodes to a single outgoing node implicitly contain a lower-dimensional cell serving as frontier between those cells or nodes that are exclusive to a single generatex and those that belong to several generatexes.

These key directed edges are hereafter called *Poincaré edges* and are denoted symbolically by pairs of ingoing and outgoing node labels:

$$\bar{E} = \langle \text{ingoing node label} \mid \text{outgoing node label} \rangle.$$

Notice that a joining locus gives rise to at least two Poincaré edges, reflecting the fact that the same outgoing top-cell/node is reached from two or more adjacent top-cells/nodes.

The terminology is chosen to emphasize the role of these directed edges as transverse dynamical interfaces: they mark regions where distinct directed paths become indistinguishable, in close analogy with the role played by Poincaré sections in classical dynamics.

C. Poincaré-edge operator

The *Poincaré-edge operator* is defined as

$$\mathcal{P} : C_{\mathcal{G}}(\mathcal{T}) \longrightarrow \bar{E}^*,$$

where \bar{E}^* denotes the set of all finite ordered sequences of Poincaré edges in \mathcal{T} .

Given a directed path p , the operator $\mathcal{P}(p)$ returns the ordered list of joining directed edges along p , in the order induced by the path, discarding all other directed edges. Thus, operationally, \mathcal{P} contracts a directed path onto the Poincaré edges it traverses.

D. Path templex

The *path templex* associated with a templex \mathcal{T} is the algebraic structure

$$T_{\bullet}(\mathcal{T}) = ((C_{\bullet}(\mathcal{B}), \partial), (C_{\mathcal{G}}(\mathcal{T}), \mathcal{P})),$$

where $C_\bullet(\mathcal{B})$ denotes the chain complex associated with a BraMAH complex \mathcal{B} , and $C_{\mathcal{G}}(\mathcal{T})$ denotes the collection of directed paths in the associated graph \mathcal{G} .

The notion of path complex introduced here should not be confused with that of a directed chain complex, nor with the dihomology framework developed in directed algebraic topology [8–11].

In the present construction, the underlying chain complex $C_\bullet(\mathcal{B})$ remains entirely classical: no causal direction is assigned to chains or to the boundary operator ∂ , and no homological theory is modified or replaced.

Causal direction is encoded exclusively by directed paths and by the Poincaré–edge operator acting on them. The algebraization preserves a separation between the structure visited by the flow and the flow upon it, without decoupling them.

E. The generatex quotient

Let $Z_{\mathcal{G}}$ denote the set of directed cycles, i.e., of closed directed paths, in the digraph \mathcal{G} . Two directed cycles in \mathcal{G} are said to be equivalent if and only if they have the same image under the Poincaré–edge operator. This equivalence relation induces the quotient

$$Z_{\mathcal{G}}/\sim,$$

whose elements are called *generatexes*. Equivalently, generatexes are the equivalence classes of $Z_{\mathcal{G}}$ under this relation.

This construction mirrors the classical algebraic–topological pipeline: directed paths play the role of chains, the Poincaré–edge operator extracts boundary–type causal information, and generatexes arise as a quotient of directed cycles by this operator.

A summary of the formal correspondences is provided in Table I, where X is a topological space and X^\uparrow a directed topological space.

Cell complex K	Templex $\mathcal{T} = (\mathcal{B}, \mathcal{G})$
X	X^\uparrow
$C_\bullet(K)$	$C_\bullet(\mathcal{B}), C_{\mathcal{G}}$
∂	∂, \mathcal{P}
$Z_k(K)$	$Z_k(\mathcal{B}), Z_{\mathcal{G}}$
$H_k(K)$	$H_k(\mathcal{B}), \text{Gen}(\mathcal{T})$

TABLE I. Algebraization of a cell complex and of a templex.

IV. FUNCTORIAL INVARIANTS

A category is specified by a collection of objects and morphisms equipped with identity arrows and an associative notion of composition. A functor is a structure–preserving map between categories: it sends objects to

objects and morphisms to morphisms, preserving identities and composition. Thereby, a functor provides a way to translate one type of mathematical structure into another.

In classical algebraic topology, the homology functor translates a topological space into abelian groups encoding its homological features. This correspondence is represented by the following commutative diagram, where the homology functor maps each chain complex to its homology groups:

$$\begin{array}{ccccc}
 \mathbf{Top} & \longrightarrow & \mathbf{Ch} & \longrightarrow & \mathbf{Ab} \\
 \\
 X & \longrightarrow & C_\bullet(X) & \longrightarrow & H_k(X) \\
 \downarrow & & \downarrow & & \downarrow \\
 Y & \longrightarrow & C_\bullet(Y) & \longrightarrow & H_k(Y)
 \end{array}$$

The category \mathbf{Ch} has graded abelian groups endowed with a boundary operator as objects, and degree–preserving morphisms commuting with the boundary operator as arrows.

In directed algebraic topology, the category \mathbf{dTop} consists of directed spaces and direction–preserving maps. In this setting, classical cell complexes and chain algebras are replaced by templexes and algebras of directed paths.

Let us denote by \mathbf{Pa} the category whose objects are directed path semigroups endowed with the Poincaré–edge operator, and whose morphisms are semigroup homomorphisms commuting with the Poincaré–edge operator.

At this point, recall that a forgetful functor maps an object to a structure obtained by discarding part of the object’s data, while keeping the remaining structure and the induced morphisms. Two forgetful functors arise naturally from the above commutative diagram.

The first one,

$$U_{\mathcal{G}} : \mathbf{dTop} \longrightarrow \mathbf{Ch},$$

forgets the digraph component and retains only the underlying chain complex, thereby recovering the classical functorial chain. The second one,

$$U_{\mathcal{B}} : \mathbf{dTop} \longrightarrow \mathbf{Pa},$$

forgets the chain complex structure but preserves the directed path algebra together with the Poincaré–edge operator, which inherits properties derived from the prior construction of the BraMAH complex. It may seem a detail, but it is not: the inherited properties are being translated into the non–graded category \mathbf{Pa} . This feature is due to the fact that causal direction in the templex–based framework does not propagate to lower–dimensional cells, but remains confined to transitions between top–cells.

The categories \mathbf{Ch} and \mathbf{Pa} are scaffold–dependent. Functorial invariants must now condense the scaffold–independent properties. The generatex functor,

$$F_{Gen} : \mathbf{Pa} \longrightarrow \mathbf{Sem},$$

maps each path structure to the semigroup generated by its generatexes. It plays for directed paths in a templex a role conceptually parallel to that played by the homology functor for chain complexes. The resulting composition,

$$F_{Gen} \circ U_B : \mathbf{dTop} \longrightarrow \mathbf{Sem},$$

defines a functorial construction parallel to the classical homology theory, but defining causal equivalence classes, and leading to a semigroup encoding its intrinsic directed invariants.

$$\begin{array}{ccccc} X^\uparrow & \longrightarrow & T_\bullet(X^\uparrow) & \longrightarrow & (H_k(X), Gen(X^\uparrow)) \\ \downarrow & & \downarrow & & \downarrow \\ Y^\uparrow & \longrightarrow & T_\bullet(Y^\uparrow) & \longrightarrow & (H_k(Y), Gen(Y^\uparrow)) \end{array}$$

The new functorial chain sends directed spaces onto directed spaces, preserving the generatex structure with its associated Poincaré edges. It provides a functorial framework in which the classical directionless invariants, i.e., the homology groups, as well as the directed invariants, i.e., the generatex semigroups, coexist.

While homology group generators are classes of chains encircling voids in a topological space, generatex semigroups are classes of top-paths circling around joining loci. The analogies between the two kinds of functorial invariants are summarized in Table II.

Level	Directionless	Directed
Spaces	Topological spaces $X \in \mathbf{Top}$	Directed spaces $X^\uparrow \in \mathbf{dTop}$
Algebraic encoding	Chain complex algebra $(C_\bullet, \partial) \in \mathbf{Ch}$	Directed path algebra $(C_G, \mathcal{P}) \in \mathbf{Pa}$
Algebraic invariants	Homology groups $H_k(X) \in \mathbf{Ab}$	Generatex semigroups $Gen(X^\uparrow) \in \mathbf{Sem}$

TABLE II. Categorical correspondences...

From a categorical perspective, a *pushout* provides a canonical way of gluing two algebraic structures along a common substructure. Accordingly, bonds between generatexes admit a natural pushout interpretation. Let $Gen(X^\uparrow) \in \mathbf{Sem}$ denote the generatex semigroup associated with a directed space X^\uparrow . Given two generatex semigroups $G_1, G_2 \leq Gen(X^\uparrow)$, their *bond* is defined as the common subsemigroup

$$B_{12} = G_1 \cap G_2.$$

The canonical inclusions $B_{12} \hookrightarrow G_1$ and $B_{12} \hookrightarrow G_2$ define

a cospan in \mathbf{Sem} , and hence a pushout diagram

$$\begin{array}{ccc} B_{12} & \xleftarrow{i_1} & G_1 \\ \downarrow i_2 & & \downarrow j_1 \\ G_2 & \xrightarrow{j_2} & G_1 \sqcup_{B_{12}} G_2 \end{array} \quad (\text{in } \mathbf{Sem}),$$

which formalizes the gluing of generatex subsemigroups along their bond.

The cardinality of the index set labeling the intersection, given here by $|\{1, 2\}| = 2$, is termed the *valence* of the bond, that is, the number of indistinguishable generatexes sharing that portion of the dynamics. The term *valence* refers to the analogy with valence electrons in chemistry, to emphasize that bonds encode how the fundamental dynamical units combine through the gluing of generatexes, in the same spirit as introduced in the decomposition into fundamental units of the templex [14, 17].

Pushouts capture the local loss of causal distinguishability induced by the flow on the top-level of the structure. Outside the bond, generatexes remain distinct; within it, trajectories are structurally identified. Such alternations between separation and identification provide a natural categorical description for the finite-time topology of chaos. They are also useful in identifying commonalities and differences between *topological modes of variability (TMVs)* in individual trajectories of the associated dynamics [17].

V. APPLICATIONS

Two examples are provided to illustrate how the semigroup structure and functorial invariants emerge from experimental [5] and numerical [17] data.

The first example is a speech signal used to show that the topology of short and noisy time series can actually be retrieved through homologies [5]. The templex and its directed invariants for this dataset are computed here for the first time. While the correspondence between the embedded trajectory and a three 1-hole structure cannot be taken as an indication of chaoticity, the directed invariants obtained through the generatex functor can, as shown below.

The second example is a numerical simulation of a conceptual four-dimensional model that captures key processes of the large-scale ocean circulation [17]. This example is revisited to illustrate how functorial invariants can be handled in nonautonomous settings. The TMVs introduced in this setting as metric manifestations of generatexes can be used in the detection of the *topological tipping points (TTPs)* found in Ref. [20].

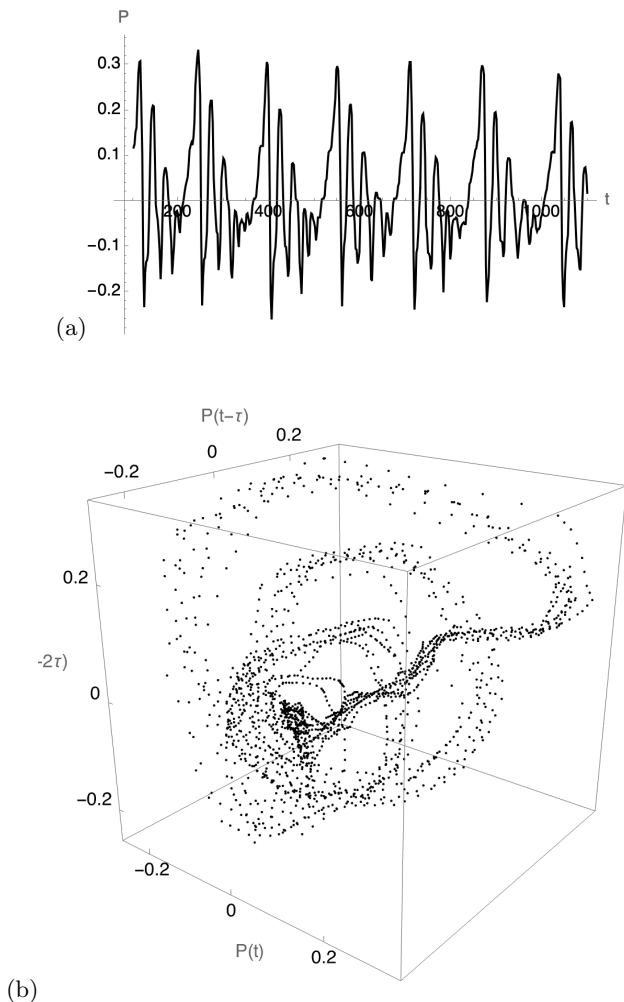


FIG. 1. The time series of the pressure fluctuation values (in arbitrary units) as a function of their position in the data file. (a) The entire time series for $t = 0.147$ sec. (b) The three-dimensional time-delay embedding of the time series, with $\tau = 5$.

A. A speech signal

The speech signal analyzed here corresponds to pressure fluctuations generated by the airflow through the vocal folds during vowel production.

Vowel sounds result from a self-sustained oscillatory regime in which vocal-fold motion couples with the airflow driven by subglottal pressure. The vowel quality is further shaped by the supraglottal vocal tract, which acts as an acoustic resonator. The governing equations are inherently nonlinear, involve delayed feedback mechanisms, and are therefore known to produce complex and sometimes chaotic dynamical signatures.

Here we reconsider the dataset in Ref. [5], namely, the signal for vowel “a” as pronounced in Spanish. The time series and its time-delay embedding are displayed in Figs. 1(a,b). The file contains 1183 points corresponding to a total interval of $t \approx 0.147$ s, with the measurements

taken at 8 000 samples per second.

The analysis is conducted by applying the forgetful functor $U_{\mathcal{B}}$, since homological properties were already discussed in Ref. [5]. The BraMAH complex analysis yields a structure with three 1-holes and two junction loci. The 1-cells (hinges) shared by more than three 2-cells are $J_1 = [4, 5]$ and $J_2 = [10, 11]$, using the same 0-cell labels as in Ref. [5] (not shown here). The new aspect of the present work lies in the directed part of the templex, which reveals three distinct generatex classes forming the generatex semigroups.

Each generatex is expressed as a cycle of the digraph, whose node indices correspond to the labels of point subsets forming 2-cells, as shown in Fig. 2(a).

$$\begin{aligned} G_1 &= \{7 \rightarrow 17 \rightarrow 9 \rightarrow 18 \rightarrow 20 \rightarrow 21 \rightarrow 15 \rightarrow 16\}, \\ G_2 &= \{7 \rightarrow 17 \rightarrow 9 \rightarrow 10 \rightarrow 11 \rightarrow 13 \rightarrow 14 \rightarrow 15 \rightarrow 16\}, \\ G_3 &= \{1 \rightarrow 2 \rightarrow 3 \rightarrow 4 \rightarrow 5 \rightarrow 6 \rightarrow 7 \rightarrow 17 \rightarrow 9 \rightarrow 22 \\ &\quad \rightarrow 23 \rightarrow 25 \rightarrow 19 \rightarrow 12\}. \end{aligned}$$

These three generatexes intersect in the following bonds, defined as common subsemigroups of the generatex semigroup:

$$\begin{aligned} B_{123} &= G_1 \cap G_2 \cap G_3 = \{7 \rightarrow 17 \rightarrow 9\}, \\ B_{12} &= G_1 \cap G_2 = \{15 \rightarrow 16 \rightarrow 7\}. \end{aligned}$$

which can also be identified in the digraph; see Fig. 2(b).

When the generatexes are superposed in a single digraph, bonds appear as multiple directed edges, one contributed by each generatex. The *valence* of the bond is given by the number of parallel edges: 3 in B_{123} and 2 in B_{12} .

To make the causal boundaries underlying these directed cycles explicit, we apply the Poincaré-edge operator \mathcal{P} to each generatex. This operator filters the directed paths and retains only the edges of the form $\langle \text{IN} \mid \text{OUT} \rangle$, which go through the joining (top-1)-cells of the BraMAH complex.

$$\begin{aligned} \mathcal{P}(G_1) &= \{\langle 21 \mid 15 \rangle, \langle 16 \mid 7 \rangle\}, \\ \mathcal{P}(G_2) &= \{\langle 14 \mid 15 \rangle, \langle 16 \mid 7 \rangle\}, \\ \mathcal{P}(G_3) &= \{\langle 6 \mid 7 \rangle\}. \end{aligned}$$

Poincaré edges $\langle 14 \mid 15 \rangle$ and $\langle 21 \mid 15 \rangle$ are associated with J_1 , while $\langle 16 \mid 7 \rangle$ and $\langle 6 \mid 7 \rangle$ are associated with J_2 .

In this example, each generatex class encircles one of the three one-dimensional holes detected in the homological analysis. The 1-holes surround regions of phase space that remain unvisited, while generatexes are closed paths around the joining loci.

Fig. 2(c) shows the generatexes visited by the trajectory as a function of time, that is, the itinerary induced by the dynamics on the generatex decomposition of the templex. The signal alternates irregularly between the three generatexes G_1, G_2, G_3 , with strongly variable residence times: approximately 319.9 time units in G_1 , 130.0 in G_2 , and 513.6 in G_3 . While transitions $G_3 \rightarrow G_1$

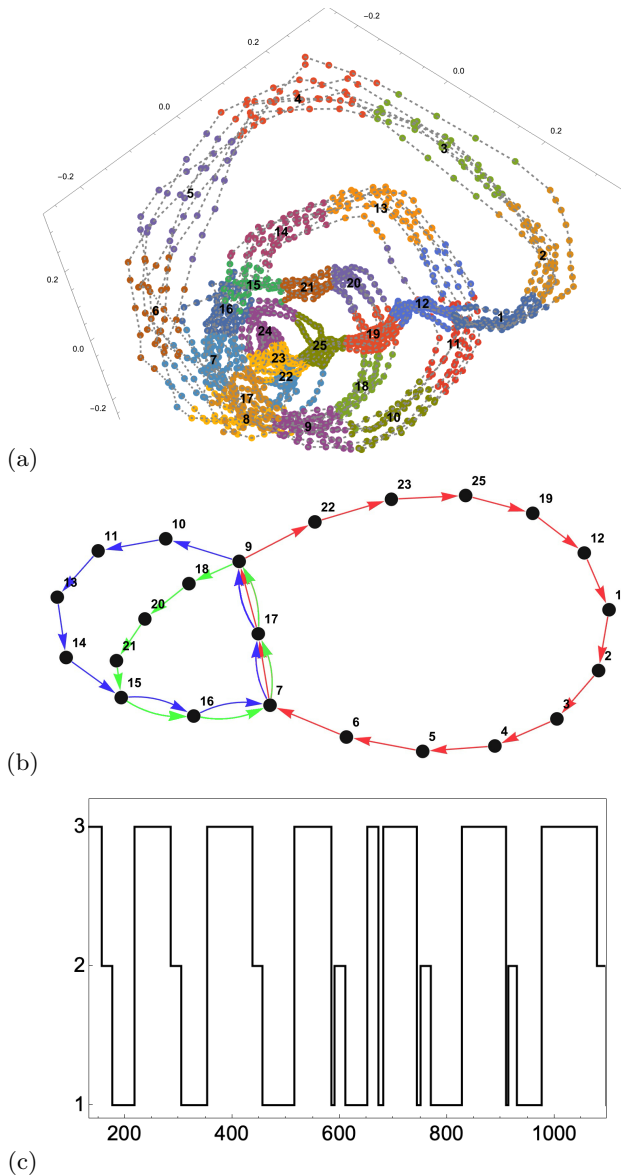


FIG. 2. Forgetful functor analysis of the time series in Fig. 1. (a) Point cloud segmented into the 2-cells of the BraMAH complex (faces are omitted for clarity). (b) Directed multi-graph obtained as the union of the three generatexes G_1 in green, G_2 in blue, and G_3 in red; parallel edges indicate bonds—the triple one B_{123} and the double one B_{12} . Removing parallel edges yields the digraph of the templex. (c) Generatex visitation sequence extracted from the time series [μsec].

and self-concatenations $G_1 \rightarrow G_1$ dominate, the sequence $G_3 \rightarrow G_2 \rightarrow G_1$ appears only intermittently.

This behavior provides an operational indication of finite-time irregularity that goes beyond what can be inferred from directionless algebraic topology alone. While undirected invariants such as junction loci are, at least, highly suggestive of possibly transient chaos, they do not encode the causal structure of the dynamics.

Within the functorial framework, this behavior is char-

acterized at the topological level by the existence of joining loci and generatexes. When these structures are genuine and not artifacts of the construction of the BraMAH complex from data, the sequence induced by a trajectory is expected to exhibit a non-periodic visiting pattern, with irregular residence times. Notice that this is not imposed as a defining criterion, but arises as a metric manifestation of the underlying topological structure.

B. Wind-driven double gyre

Understanding the effects of time-dependent forcing on intrinsic ocean variability is crucial for modeling climate variability in general. This section presents a numerical simulation reported in Ref. [17] based on an intermediate complexity model [21] for the streamfunction of the wind-driven ocean circulation in midlatitudes [22].

In the case of aperiodic wind-stress forcing, three junction loci—one joining and two splitting loci—are detected. Note that cells are renumbered here as $\gamma_i \mapsto i$ ($i = 1, \dots, 6$) and $\sigma_j \mapsto 6 + j$ ($j = 1, \dots, 16$).

Six generatexes are identified:

$$G_1 = \{1 \rightarrow 2 \rightarrow 3 \rightarrow 4 \rightarrow 1\},$$

$$G_2 = \{1 \rightarrow 2 \rightarrow 3 \rightarrow 5 \rightarrow 6 \rightarrow 17 \rightarrow 18 \rightarrow 19 \rightarrow 20 \rightarrow 21 \rightarrow 22 \rightarrow 1\},$$

$$G_3 = \{1 \rightarrow 2 \rightarrow 3 \rightarrow 5 \rightarrow 6 \rightarrow 12 \rightarrow 13 \rightarrow 1\},$$

$$G_4 = \{1 \rightarrow 2 \rightarrow 3 \rightarrow 5 \rightarrow 6 \rightarrow 7 \rightarrow 8 \rightarrow 1\},$$

$$G_5 = \{1 \rightarrow 2 \rightarrow 3 \rightarrow 5 \rightarrow 6 \rightarrow 9 \rightarrow 10 \rightarrow 11 \rightarrow 1\},$$

$$G_6 = \{1 \rightarrow 2 \rightarrow 3 \rightarrow 5 \rightarrow 6 \rightarrow 14 \rightarrow 15 \rightarrow 16 \rightarrow 1\}.$$

The directed multi-graph obtained from the union of the six generatexes is shown in Fig. 3(a).

The six generatexes intersect in two bonds, defined as common subsemigroups of the generatex semigroup:

$$B_{123456} = \bigcap_{i=1}^6 G_i = \{1 \rightarrow 2 \rightarrow 3\},$$

$$B_{23456} = \bigcap_{i=2}^6 G_i = \{1 \rightarrow 2 \rightarrow 3 \rightarrow 5 \rightarrow 6\}.$$

The valence of the bonds, given by the number of parallel edges, is 6 for B_{123456} and 5 for B_{23456} . Applying the Poincaré-edge operator \mathcal{P} to each generatex, we obtain:

$$\mathcal{P}(G_1) = \{\langle 4 | 1 \rangle\},$$

$$\mathcal{P}(G_2) = \{\langle 22 | 1 \rangle\},$$

$$\mathcal{P}(G_3) = \{\langle 13 | 1 \rangle\},$$

$$\mathcal{P}(G_4) = \{\langle 8 | 1 \rangle\},$$

$$\mathcal{P}(G_5) = \{\langle 11 | 1 \rangle\},$$

$$\mathcal{P}(G_6) = \{\langle 16 | 1 \rangle\}.$$

all of them containing the joining locus at the 1-cell labeled $[0, 1]$ in Fig. 14(a) of Ref. [17]. The generatex visitation sequence versus time is shown in Figure 3(b). Here,

encode the non-equivalent ways of circling around the non-manifold loci of the support.

The speech example reconsidered here is the same voice signal used to illustrate the extension of BraMAH analysis more than two decades ago [5]. It is the first templex constructed from a fully experimental signal and the first application of the framework to voice dynamics. The directed invariants provide an operational signature of irregularity and finite-time chaoticity that remained undetermined with homologies alone. The detection of three generatex classes and two bonds of different valence illustrate how functorial invariants operate in practice.

The climatic example shows how the formalism works with a four-dimensional phase space and non-autonomous settings [22]. Within the categorical framework, Topological Modes of Variability (TMVs), the metric manifestation of generatex classes, acquire a precise interpretation through the algebra of directed paths. This clarifies why the TMVs of an individual solution must be concatenated in time, rather than superposed, as is the case in other approaches to the decomposition of dynamically generated time series [17].

Coexistence of several TMVs for a single time may obviously arise in ensemble realizations of a chaotic system, providing a topological interpretation of changes in

the statistical moments of such a system in the presence of time-dependent forcing [23]. Topological tipping occurs for those instants in which the set of coexisting TMVs changes — e.g., a TMV disappears or a new TMV emerges — thus providing a deeper topological interpretation of such tipping.

To conclude, this article presents a functorial formulation for chaos topology. Placing the templex within the broader mathematical framework of category theory discloses why homology must not be replaced by directed homology, what kind of object the templex is, and why two related but distinct functorial chains are required to translate chaotic dynamics into a complete set of topological invariants. This formulation brings together — while keeping them distinct — two notions that are traditionally difficult to reconcile: time and structure.

Acknowledgments The author wishes to thank Michael Ghil for careful reading and insightful discussions, and Christophe Letellier for several exchanges on templates. Funds from the ANR project TeMPlex ANR-23-CE56-0002 are acknowledged.

-
- [1] J. S. Birman and R. F. Williams, *Topology* **22**, 47 (1983).
 [2] R. Gilmore, *Rev. Mod. Phys.* **4**, 1455 (1998).
 [3] M. Lefranc, *Physical Review E—Statistical, Nonlinear, and Soft Matter Physics* **74**, 035202 (2006).
 [4] S. Mangiarotti *et al.*, *Habilitation to direct Researches, Université de Toulouse* **3** (2014).
 [5] D. Sciamarella and G. B. Mindlin, *Phys. Rev. Lett.* **82**, 1450 (1999).
 [6] D. Sciamarella and G. B. Mindlin, *Phys. Rev. E* **64**, 036209 (2001).
 [7] G. D. Charó, G. Artana, and D. Sciamarella, *Phys. D* **405**, 132371 (2020).
 [8] M. Grandis, *Cahiers de Topologie et Géométrie Différentielle Catégoriques* **44**, 281 (2003).
 [9] E. Goubault, in *Proceedings of the Workshop on Geometry and Topology in Concurrency Theory*, Vol. 81 (Electronic Notes in Theoretical Computer Science, 2003) pp. 1–39.
 [10] P. Gaucher, *Mathematical Structures in Computer Science* **15**, 409 (2005).
 [11] M. Grandis, *Directed Algebraic Topology: Models of Non-Reversible Worlds*, New Mathematical Monographs, Vol. 13 (Cambridge University Press, Cambridge, 2009).
 [12] G. D. Charó, C. Letellier, and D. Sciamarella, *Chaos: An Interdisciplinary Journal of Nonlinear Science* **32**, 083108 (2022).
 [13] D. Sciamarella and G. D. Charó, in *Topological Methods for Delay and Ordinary Differential Equations: With Applications to Continuum Mechanics* (Springer, 2024) pp. 191–211.
 [14] C. Mosto, G. D. Charó, C. Letellier, and D. Sciamarella, *Chaos: An Interdisciplinary Journal of Nonlinear Science* **34** (2024).
 [15] S. Eilenberg and S. M. Lane, *Transactions of the American Mathematical Society* **58**, 231 (1945).
 [16] S. M. Lane, *Categories for the Working Mathematician*, Graduate Texts in Mathematics, Vol. 5 (Springer, 1971).
 [17] G. D. Charó, D. Sciamarella, J. Ruiz, S. Pierini, and M. Ghil, *Chaos: An Interdisciplinary Journal of Nonlinear Science* **XX** (2025).
 [18] G. D. Charó, G. Artana, and D. Sciamarella, *J. Fluid Mech.* **923**, A17 (2021).
 [19] H. Edelsbrunner and J. L. Harer, *American Mathematical Society* (2010), see Chapter III for Čech and Vietoris–Rips complexes.
 [20] G. D. Charó, M. D. Chekroun, D. Sciamarella, and M. Ghil, *Chaos: An Interdisciplinary Journal of Nonlinear Science* **31**, 103115 (2021).
 [21] M. Ghil and V. Lucarini, *Reviews of Modern Physics* **92**, 035002 (2020).
 [22] S. Pierini and M. Ghil, *Sci. Rep.* **11**, 1 (2021).
 [23] B. Maraldi, H. A. Dijkstra, and M. Ghil, *Chaos: An Interdisciplinary Journal of Nonlinear Science* **35**, 10.1063/5.0253103 (2025).